Physics-Informed Data-Driven Approaches to State of Health Prediction of Maritime Battery Systems

Azzeddine Bakdi[1], Maximilian Bruch [2], Qin Liang[3, 4], Erik Vanem[3, 5]

[1] *Corvus Energy, Porsgrunn, Norway*
abakdi@corvusenergy.com

[2] *Fraunhofer ISE, Freiburg, Germany*
maximilian.bruch@ise.fraunhofer.de

[3] *DNV Group Research & Development, Høvik, Norway*
Qin.Liang@dnv.com
Erik.Vanem@dnv.com

[4] *Department of Ocean Operations and Civil Engineering, Norwegian University of Science and Technology, Ålesund, Norway*
qinlia@stud.ntnu.no

[5] *Department of Mathematics, University of Oslo, Oslo, Norway*
erikvan@math.uio.no

Abstract

Battery systems are increasingly being used for powering ocean going ships, and the number of fully electric or hybrid ships relying on battery power for propulsion and maneuvering is growing. In order to ensure the safety of such electric ships, it is of paramount importance to monitor the available energy that can be stored in the batteries, and classification societies typically require that the state of health (SOH) of the batteries can be verified by independent tests annual capacity tests. However, this paper discusses physics-informed data-driven approaches to online diagnostics for state of health monitoring of maritime battery systems based on a combination of physical knowledge, physic-based models, insights from extensive characterization tests and operational sensor data collected from the batteries during actual operation. This represents an alternative approach to the annual capacity tests for electric ships that is found to be sufficiently robust and accurate under certain conditions. Previous attempts with purely data-driven models, including both cumulative and snapshot models, semi-supervised learning and simple models based on the state of charge did not achieve the required reliability and accuracy for them to be utilized in a ship classification perspective, as presented at previous PHM conferences. However, preliminary results from the physics-informed data-driven method presented in this paper indicate that it can be relied on for independent verification of state of health as an alternative to physical tests. It has been tested on battery cells cycled in laboratory degradation tests as well as on field returns from batteries onboard ships in service. Notwithstanding, further validation and verification of the method is recommended to further build confidence in the model predictions.

Erik Vanem et al. This is an open-access article distributed under the terms of the Creative Commons Attribution 3.0 United States License, which permits unrestricted use, distribution, and reproduction in any medium, provided the original author and source are credited.

1. Introduction

The safety of battery-powered ships is important, and classification societies have rules for the safe design, construction and operation of such ships. One crucial aspect of the safety of electric ships is to ensure that sufficient energy is stored in the batteries to cover the required demand for the intended operation (Hill et al., 2015). Loss of propulsion power in a critical situation can lead to serious accidents such as collision or grounding. Therefore, robust estimation and prediction of the actual available energy of a battery is crucial for ship safety.

Batteries are aging and the energy storage capacity degrades over time. The aging process affects both the amount of charge that can be stored and the available power. Most maritime battery systems are designed with an expected lifetime of 10 years and end of life is typically defined as State of

Health (SOH) = 70-80%, where SOH stands for the ratio of remaining capacity to initial capacity (in %). Ships, on the other hand, are typically design for 25-30 years. Hence, batteries are expected to approach their end of useful life (EOL) long before the end of the operational life of the vessels. In such a context, reliable estimation of SOH will become increasingly important as the battery systems approaches its EOL and making correct decisions on remaining useful life (RUL) will have great financial and safety implications.

Currently within the maritime Industry, the commonly adopted approach for evaluating the real-time capacity of an onboard battery system is by considering the State of Charge (SOC) and the State of Health (SOH): Available energy = Initial Capacity x SOC x SOH. A major part of such an estimation will be a reliable evaluation of the battery State of Health, which is challenging. Currently, battery suppliers are required to have an SOH estimation algorithm and to regularly verify the SOH annually through in-situ capacity testing. From a practical point of view, the annual capacity test is time consuming and typically requires that the ship is taken out of operation for one full day. Moreover, the accuracy of the test is questionable due to several factors influencing the results, such as variability in loads, temperatures and Depth of Discharge (DOD). As ship-to-shore connectivity has improved immensely over the past few years it is natural to evaluate whether a sensor-based monitoring system can used for diagnostics in order to both reduce downtime for the operator and improve the quality of the SOH verification.

A review of different methods for data-driven diagnostics of maritime battery systems were presented in Vanem, Bertinelli Salucci, et al. (2021); Vanem, Alnes, & Lam (2021). According to this review, data-driven methods for estimating battery capacity can be categorized into a few generic type of approaches. Additionally, a distinction was made between models that rely on the complete loading history of the batteries in order to estimate current state of health – cumulative methods – and what was referred to as snapshot methods, where state of health and capacity can be estimated based on only snapshots of the data. Other recent reviews of state of the art methods for condition monitoring and data-driven state of health prediction can be found in e.g. Berecibar et al. (2016); Ungurean et al. (2017); Xiong et al. (2018); Lipu et al. (2018); Pastor-Fernández et al. (2019); Li et al. (2019); Huixin et al. (2020).

Some recent approaches involving the combination of data and equivalent circuit models (ECM) for estimation of state of health are reported in e.g. Chen et al. (2023); Yang et al. (2023); Hu & Qian (2024), see also the overview presented in Shu et al. (2021). Previous models based on open circuit voltage (OCV) for state of health prediction are presented in e.g. Weng et al. (2014); Bian et al. (2020, 2022); Noh et al. (2023), see also Yu et al. (2018); Meng et al. (2020); Wang et al. (2023); Zhou et al. (2024) for related work on estimating the OCV curve.

This paper presents physics-informed data-driven approaches to state of health modeling for maritime battery systems. The overall idea is to use sensor data from batteries to learn the degradation state of the batteries without the need for specific testing or characterization cycles. If successful, data-driven approaches may replace the need for annual capacity testing to verify SOH according to class rules. This paper extends previous attempts that were purely data-driven. As it turned out, purely data-driven approaches left something to be desired in terms of accuracy and computational efficiency to be recommended for implementation onboard maritime batteries, either for cumulative methods or snapshot methods, as outlined in e.g. Liang et al. (2023); Grindheim et al. (2024); Vanem, Bruch, et al. (2023); Bertinelli Salucci et al. (2023); Vanem, Liang, Ferreira, et al. (2023). However, by combining physics-based insight with data-driven methods, it is possible to achieve reasonable results, as outlined in this paper. Hence, this paper continues the story from previous papers presented at the PHM conference Vanem, Alnes, & Lam (2021); Vanem et al. (2022); Vanem, Liang, Ferreira, et al. (2023), and presents the final chapter with the final recommendations.

It is important to note that different approaches set different requirements for the data. For example, most approaches require training data to train the data-driven models, whereas some approaches can do without training data. If training data are required, they obviously need to be representative of typical operational data, and should preferably correspond to identical cells as the system it should be applied to. This is among the considerations that need to be made when comparing and recommending which models to use for data-driven classification of the batteries. Other factors to consider, apart from the predictive performance, include amount of data needed, the sensitivity to missing data and the computational costs.

The main contribution from this paper is the presentation of a novel physics-informed data-driven approach that combines physical insight with operational data to provide reliable state of health estimation of maritime battery systems based on sensor data and without the need for special tests.

2. BATTERY DATASETS

Different sets of data have been available for analysis and modeling in the project. These include laboratory data generated by the project, proprietary data from actual ships in operation and some publicly available datasets. For a more complete description of these datasets, references is made to data descriptions in a previous PHM conference paper Vanem, Liang, Ferreira, et al. (2023), and a brief summary is presented in the following.

2.1. Laboratory Cycling Data

Three different types of battery cells have been subject to laboratory cycling tests in order to generate degradation data for the cells. Two types of cylindrical 18650 cells, i.e. energy cells (henceforth denoted DDE; nominal capacity 3.5 Ah) and power cells (henceforth denoted DDP; nominal capacity 2.5 Ah), and one type of pouch cells (henceforth denoted DDF; nominal capacity 64 Ah) have been cycled according to specified test matrices. Individual cells have been cycled within specified lower and upper voltage limits, with specified charge and discharge currents, and at specified controlled temperatures. Varying these parameters yields different degradation rates. This continuous cycling is interrupted at regular intervals to perform check-ups and capacity measurements, i.e. pulse tests and charge and discharge capacity measurements by way of Coulomb counting over deep cycles at low current rates. Hence, capacities will be measured at certain points in time for all cells.

Values of current, voltage and temperature are sampled continuously, resulting in time-series of these variables throughout the experiment. From these raw measurements, different derived variables can be calculated as well, such as cumulative throughputs, cycle counts and equivalent full cycles. Measurements are obtained from a total of 81 individual cells; 35 DDE cells, 30 DDP cells and 16 DDF cells. The cells in this experiments have been charged and discharged according to a constant-current-constant voltage (CCCV) scheme: the cells are charged/discharged with constant current until the cut-off voltage, where the cells continue to charge/discharge at constant voltage with a current that gradually decreases towards zero.

2.2. Field Data From Ships in Operation

Field data from electric ships with a battery system of pouch cells of type DDF have been available for this study. These battery systems are designed with a 4-layer structure; individual *cell-pairs* connected in series make up *modules*, modules connected in series form *packs* and several packs connected in parallel make up an *array*. A ship may have one or more arrays connected in parallel as independent energy storage systems that do not communicate directly, and any combination of packs in an array can be powered off during operation. Raw data from these systems include the pack voltage and current for all packs as well as the cell voltage, temperature and State of Charge (SOC) for all cells (or rather, cell-pairs). Since modules and cell-pairs are connected in series within a pack, the current will be the same for all series elements in that pack. However, it will not be possible to distribute this current over the two cells in a series element. Hence, for all practical purposes, the cell-pairs will be considered the smallest entities of the system, i.e. cells. Moreover, whereas currents, voltages and temperatures are measured directly by sensors, SOC is a derived quantity that needs to be calculated from the other raw sensor measurements.

Operational data from 6 different ships with the same battery system on board have been available for this study. These ships include both hybrid and all-electric solutions and with different configurations (different number of arrays and packs per array). All of these systems are relatively new, without having experienced extensive degradation. Results from annual capacity tests are available, and all vessels had undergone at least two such tests by the time of this study.

Additional data from an older battery system have been analyzed in this study. These have different types of battery cells, but with the benefit of longer time histories. However, data quality is somewhat lower, and there are more and longer data gaps compared to the newer system. Data from these systems are referred to as Site A, Site B and Site C and include data from three different vessels.

3. DATA-DRIVEN STATE OF HEALTH ESTIMATION UTILIZING PHYSICAL PRINCIPLES

In this section of the paper, a description of various physics-informed data-driven approaches that have been explored in this study will be presented. They represent continuous research efforts that was made to improve on more purely data-driven methods that was found to lack in accuracy and computational efficiency, e.g. cumulative methods that are too data greedy and computationally heavy Liang et al. (2023); Grindheim et al. (2024), snapshot methods that did not achieve the desired accuracy Vanem, Bruch, et al. (2023) and reliability and semi-supervised approaches Bertinelli Salucci et al. (2023) that were tried out due to lack of training data, see also Vanem, Liang, Ferreira, et al. (2023); Vanem et al. (2024). By exploiting physical knowledge, the need for training data can also be relaxed, something of great value since reliable training data is scarce and time-consuming and expensive to generate. In this paper, two preliminary approaches will be presented before arriving at the final method that ended up being recommended and implemented for actual use on ships in operation.

All of the methods presented in this paper exploit the fundamental relationship between integrated current and change in state of charge (SOC), i.e. Coulomb counting. That is, the relationship between the total capacity Q and change in state of charge SOC of a battery between times t_1 and t_2 is described by the following equation:

$$\int_{t_1}^{t_2} \eta I(\tau) d\tau = Q \left(SOC(t_2) - SOC(t_1) \right) \tag{1}$$

where $I(\tau)$ is the battery current at time τ measured in amperes, which is defined as positive when charging and negative when discharging, and η is a unitless Coulomb efficiency factor. For simplification, $\eta \approx 1$ may be assumed.

3.1. Simple Linear Models Based on Coulomb Counting

A simple linear model based on Coulumb counting was proposed by Plett (2011), which formulated eq. 1 as a linear regression problem,

$$Y = QX + \varepsilon, \tag{2}$$

with $Y = \int_{t_1}^{t_2} \eta I(\tau) d\tau$ and $X = SOC(t_2) - SOC(t_1)$. By collecting data for Y and X the regression coefficient Q can be estimated by different methods, such as ordinary least squares (OLS) and total least squares (TLS), to yield an estimate of the total capacity of the battery. Note that the regression model does not have an intercept; when there is no current, or when the integrated current is zero, there should also not be any change in SOC. Hence, in principle, one observation of concurrent (X, Y) should be sufficient to give an estimate of the regression coefficient.

Initial attempts with a simple ordinary least squares (OLS) implementation of this method was presented in Vanem, Liang, Ferreira, et al. (2023); Vanem et al. (2024), and extended to total least squares variants in order to account for the attenuation bias in OLS Kejvalova (2022); see also Vanem, Liang, Bruch, et al. (2023) for a Bayesian implementation of this model. However, changes in loading conditions were not appropriately accounted for, leading to variable results, in particular for the operational data from ships in operation.

3.2. Ensembles of Simple Linear Models

In an attempt to remedy this, an ensemble of such simple linear models were tried out on different subsets of the data. The fundamental approach is similar as above, and the linear model for the relationship between integrated current and change in state of charge is assumed. However, rather than simply integrating the current between arbitrary time points, some more careful filtering and pre-processing is applied. In particular, different linear models are applied to segments of the charge and discharge between specified voltage ranges only. Moreover, individual estimates are obtained from pure charging and pure discharging segments only, as well as estimates from the joint charge and discharge segments. This yields various estimates of capacity/SOH for the different time periods. These can again be averaged in order to obtain one unique estimate, and two types of averaging is applied. That is, normal averaging and weighted averaging, where the weights are defined as the reciprocal of the standard deviation of the individual estimates. Hence, an estimate with a large standard deviation will get lower weight than an estimate with less uncertainty.

These battery systems are typically operated between 4.0 and 3.6 Volts (with cut-off voltages at 3.0 and 4.2 V, but hardly experiencing these voltages in normal operation), hence four voltage ranges are specified in this study:

- From 3.65 to 3.7 V
- From 3.7 to 3.8 V
- From 3.8 to 3.9 V
- From 3.9 to 4.0 V

This gives rise to potentially 8 point estimates for each time period selected: one for each voltage range for charge discharge and jointly, respectively.

The implementation of this method involves the following steps and model choices: First, one need to define the time intervals on which to do the analysis from the continuous time-series. That is, how long time periods to include data from, and how far apart they should be. In this study, data from 14 days are included with 3 months apart. Hence, 14 days snapshots every three months are used to get 3-monthly capacity estimates. Some additional filters are applied to the extracted data. First, any segments containing NA values for current, SOC or the timestamp will be ignored, since this would make the current integral and the change in state of charge unreliable. Moreover, empty segments are removed from the data. Then, charge and discharge segments within the specified voltage ranges are identified by finding the down- and up-crossing of the different voltage levels. The segments between subsequent down (up)-crossings of the upper and lower voltage level are found and this yields several partial charge and discharge segments that are analyzed with the linear model separately.

Some additional filters are applied to these subsets of the data. First, more than two up- and down-crossings are required. Then, data where the time between any two recordings are too great will be ignored. This is to ensure that correct current values are used in the integration (e.g. if two subsequent current-measurements are far apart in time, the integral could be inaccurate). For the results reported herein, the maximum lag between two consecutive measurements is set to 3 minutes (180 seconds). Finally, all segments with less than 10 observations are ignored.

Additional optional filters can be applied, e.g. filter on temperature (remove data that have experienced temperatures higher than a specified maximum temperature), filter on monotonicity (that is, ignore all segments that are not monotonic). An optional factor on C-rate is also included in the implementation, i.e. it is possible to apply a multiplicative factor to account for differences in capacity from variations in C-rate. However, in this study, temperature filters or C-rate factors have not been applied. Finally, a filter is applied that removes data-pairs where the sign of integrated current and change in state of charge are different.

One example of data extracted from an arbitrary selected cell is shown in Figure 1. Extracted segments of the discharge and charge curves between the specified voltage levels are shown to the left. The legend indicates the number of data segments with correct and incorrect sign of integrated current. In this example, there are 29 segments for discharge and 7 segments of charge, all with the same sign of change in state of charge and integrated current. Hence, all data are used in the analysis. These data gives rise to 36 datapoints to fit linear models, and three different models are fitted, as indicated in the plot to the right: one model using only the charge datapoints, one using only discharge and one model for the joint data of charge and discharge. A line corresponding to the nominal capacity of the cell is also shown in the figure.

In this way, several simple linear models yields various estimates of capacity for each cell and for each selected time period. For some time-periods, only some of the linear models are applied due to the filters applied, but for most of the time-periods there are several estimates available. Capacity estimates obtained this way are plotted over time in Figures 2, 3, 4, indicating a clear decreasing trend. In addition to the individual estimates from the different linear model, the mean and the weighted mean from all time periods are included. Also, the results from the annual capacity tests, are indicated in the plot, showing general agreement with the results from the linear model.

Note that results are generally better for vessels C and E compared to vessel A. In particular, the predicted SoH around the first annual capacity tests is considerably higher than the test results, whereas results are in better agreement for the second annual test. It is not obvious why this is the case, but one possible explanation could be related to the fact that vessel A is a hybrid vessels, whereas C and E are fully electric ferries. Presumably, all-electric vessels have more regular charge-discharge schedules and it is expected that predicting SoH based on sensor data for such vessels are easier than for hybrid vessels, with more variable charge-discharge patterns. It may also be that the results from the first annual test for this particular vessel are too low; indeed a SoH around 90% seems very low after one year of operation. In summary, it appears that predictions based on ensembles of simple linear models yields reasonable results for two of the three vessels, compared to results from annual tests. However, proper validation of such an approach is difficult without more data from ships with older systems that have experienced a higher degree of degradation and more annual test results.

One problem with the simple linear model, that can also explain the variable results, is the dependence of SOC. SOC is not directly measured, but is a derived quantity. It is assumed that SOC is less challenging to estimate accurately than SOH, but the variable results from methods relying on SOC indicate that it might not be accurate enough to be used in data-driven methods. As an attempt to remedy this, models based on the open circuit voltage will be explored next.

3.3. Methods Based on Open Circuit Voltage

The OCV based method utilizes the correlation between a battery cell's capacity and its open circuit voltage (OCV), i.e., the voltage across the cell's terminals when no electric load is connected. The OCV is increasing with SOC and its shape is not linear but has different slope changes that originate from the utilized active material in the cell (see figure 6). Apart from this useful relationship with the state of charge there is only a small influence of temperature and SOH. The obvious challenge, however, is to determine the OCV when the cell is not at rest. Therefore, an equivalent circuit model (ECM) can be deployed to describe the overpotentials and then subtract them from the measured signal. Once this has been done, all that is required is to correlate the determined OCV with the known curve and the capacity measured during operation can be correlated with the SOC. Based on this relationship the Capacity value at 100% SOC can be calculated and its relation to the nominal capacity gives the SOH. Ideally the only necessary prior knowledge for the method is the OCV-SOC-curve.

To obtain the OCV, an ECM with a serial resistance and three RC elements is used. The time constants are set to 10, 100 and 1000 seconds. The values of the resistors are matched to the monitored voltage (U_{signal}). Therefore, the voltages of a certain period of analysis (here one day) are sorted into $n_{Cgroups}$ groups according to their capacity (see example capacity section in figure 5). Then one can subtract the ECM's voltage from the measured voltage values and minimize the difference between those voltages and the average voltage value within the groups ($U_{average}$) by the adjustment of the resistance values (R_s, R_1, R_2, R_3). In other words, values are determined that reduce the voltage fluctuation within a narrow capacity range to a minimum. A least squares algorithm is used for this task.

$$\min_{R_s R_1, R_2, R_3} \sum_{i=1}^{n_{Cgroups}} |U_{i\,signal} - U_{i\,ECM} - U_{i\,average}| \quad (3)$$

The known OCV-curve is fitted to the obtained voltage, that is cleaned from the overpotential (quasi OCV). Therefore, the simulated overpotential voltage is subtracted from the measured voltage and the average in each capacity window is used to match the OCV-curve. Two parameters are defined for the approximation. One for the capacity offset, since the OCV-curve starts at a fully discharged state and the lowest capacity respectively SOC in the measured data is certainly

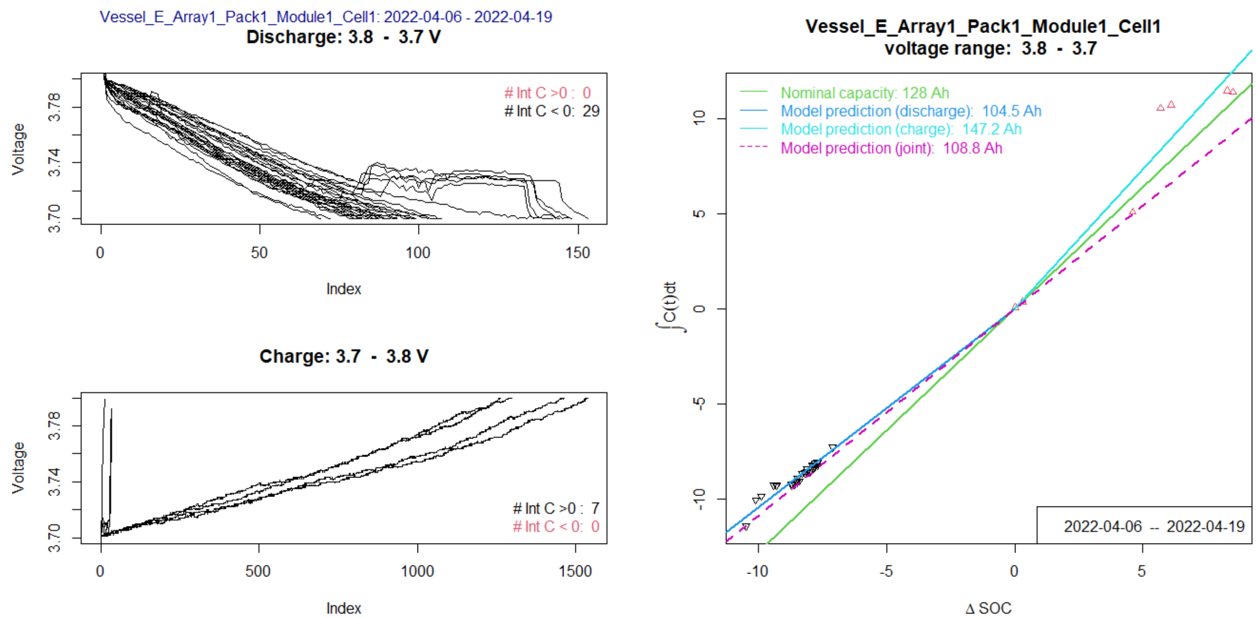

Figure 1. Example of data segments for an arbitrary cell within a specific voltage range and how it is used to fit a simple linear model. Segments of discharge and charge curves between 3.7 and 3.8 V (left) and linear models fitted to corresponding data of integrated current and change in state of charge (right)

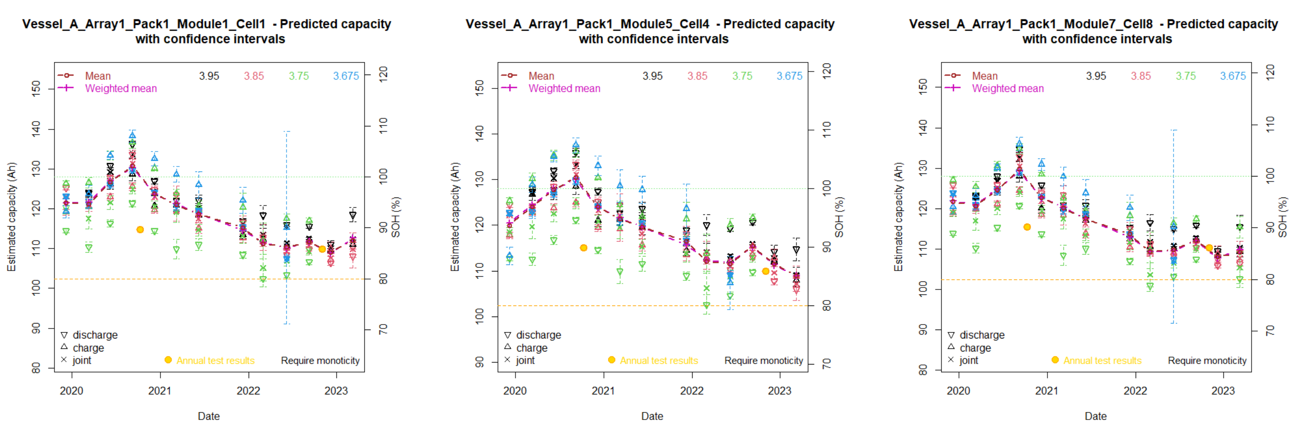

Figure 2. Examples of capacity predictions from the simple linear model for some arbitrary cells from vessel A.

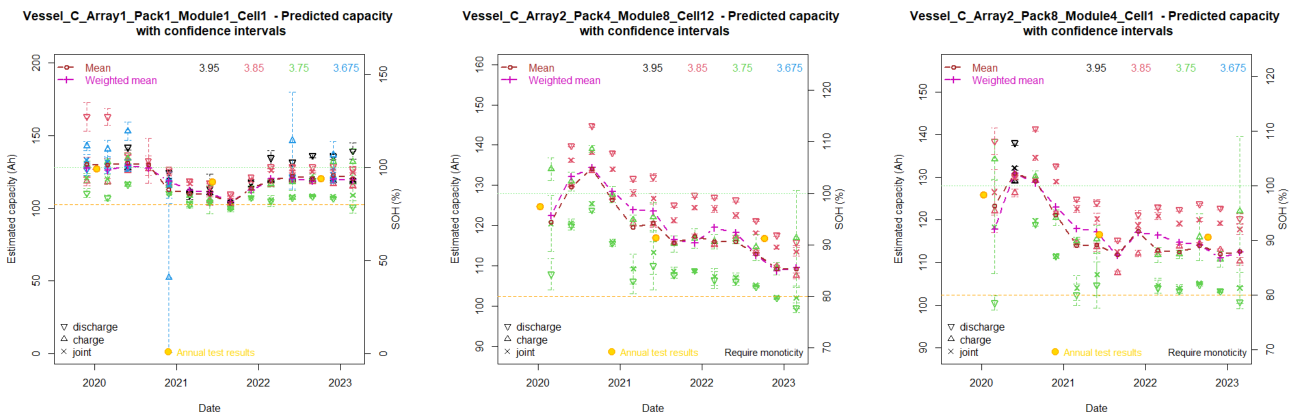

Figure 3. Examples of capacity predictions from the simple linear model for some arbitrary cells from vessel C.

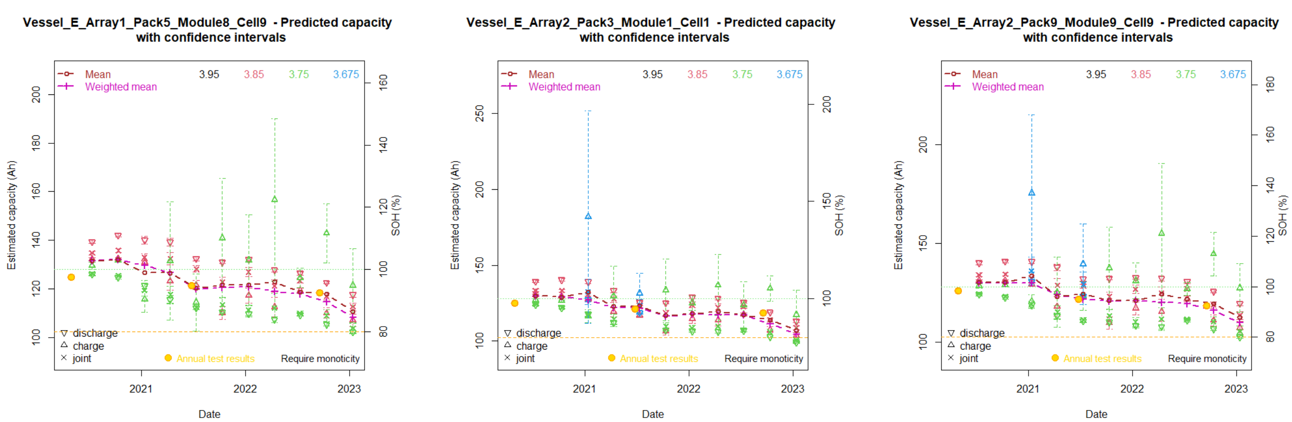

Figure 4. Examples of capacity predictions from the simple linear model for some arbitrary cells from vessel E.

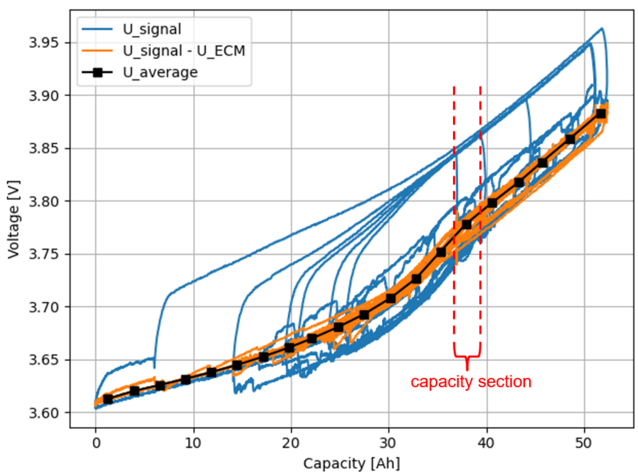

Figure 5. Measured voltage (blue line) plotted against the capacity (calculated by ampere-hour counting) of a battery cell in vessel D. The orange line represents the monitored voltage after subtracting the overpotential calculated with the approximated ECM. The black points correspond to the average of the cleaned voltages in each of the capacity sections.

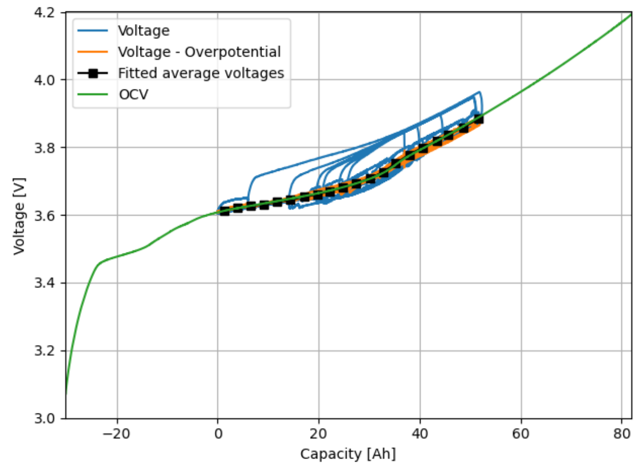

Figure 6. The known OCV (green) is matched to the obtained quasi OCV points (black). This allows one to determine the offset, but most importantly, of course, the total capacity amount.

higher. The second parameter scales the SOC range to the capacity range, where the 100% SOC value corresponds to the momentary maximum capacity of the cell. This maximum capacity value divided by the nominal capacity value gives the SOH.

$$\min_{p_1,p_2} |U_{average} - U_{OCV}(p_1, p_2)| \tag{4}$$

On closer inspection, the OCV is actually a result of the superimposed potential curves of the cell's electrodes. The cells voltage and in an idle state the OCV corresponds to the difference between the potential of the positive electrode (cathode, here NMC) and the negative electrode (anode, here graphite). Birkl et al. (2017) shows how different aging modes (loss of active material LAM at each of the electrodes and loss of lithium inventory LLI) change the shape of the OCV. Or vice versa, how the shape of the OCV can be used to obtain the LAM and LLI. Analog to the approximation with a predefined OCV-curve, the curves of the negative and positive electrodes potential (E_{NE} and E_{PE}) can be placed with two parameter (p_1, p_2 and p_3, p_4) for each electrode in such a way that the resulting OCV matches the obtained quasi OCV points.

$$U_{OCV\ EP}(p_1, p_2, p_3, p_4) = E_{PE}(p_3, p_4) - E_{NE}(p_1, p_2) \tag{5}$$

$$\min_{p_1,p_2,p_3,p_4} |U_{average} - U_{OCV\ EP}(p_1, p_2, p_3, p_4)| \tag{6}$$

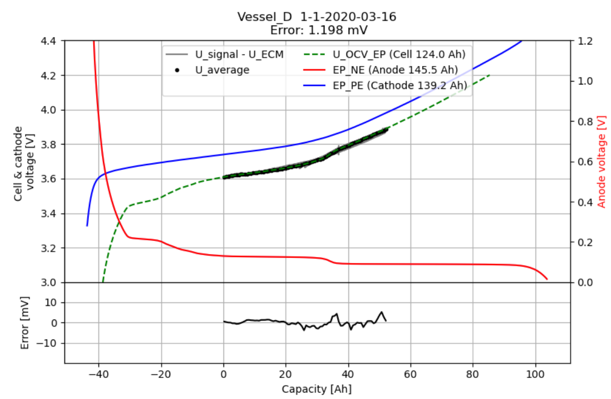

Figure 7. The electrode potentials are placed in a way that results in a match of the OCV (green dashed line) and the cleaned voltage signal. This allows not only the capacity but also LAM and LLI to be determined.

The electrode potential (EP) method is used to calculate the SOH of one specific battery cell in 4 of the vessels monitored in the project (see figure 8). In addition, the SOC-based method (total least squares) is used as a comparison. Since the values of all three SOH-estimators scatter, a running average is calculated over 21 points respectively days. If there was a gap in the recorded data or not a meaningful usage of the battery, that day or analysis interval has been excluded.

Figure 8 shows that there is a significant difference in the estimated SOH between the methods. However for vessel A and E the SOC-based and the OCV-based method have a similar, partially overlapping trend. This is surprising, since the OCV-based and EP-based method are related much closer. On the other hand, the SOC estimation is based on a Kalman filter based approach, that also uses an ECM and the SOC-OCV

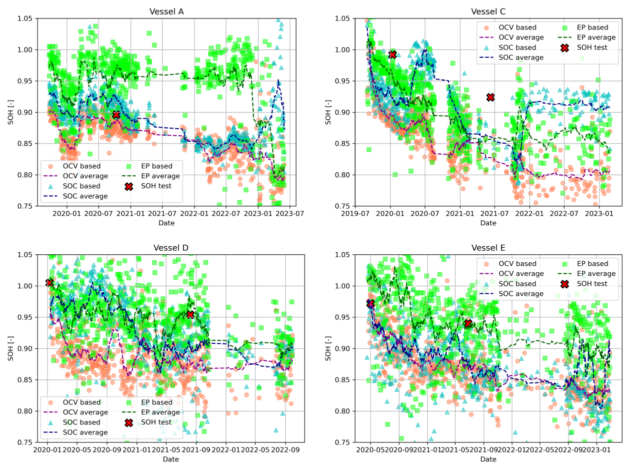

Figure 8. Overview of the SOH estimations for one cell in the various Vessels and comparison with the SOH test.

relationship to correct the ampere-hour counting, so a distant relationship can be assumed as well. Of course, the main task of the estimator is to determine the SOH and make the costly capacity test on board the ship obsolete. The comparison with those measurements show a mixed result. While the outcome of the second test of vessel D and E match the EP-based estimations, the other measurements show a meaningful deviation. Unfortunately, the other estimation procedures also show a mostly inaccurate behaviour. Another evident issue is the big spread of the daily estimates. Figure 9 gives an overview of the deviations.

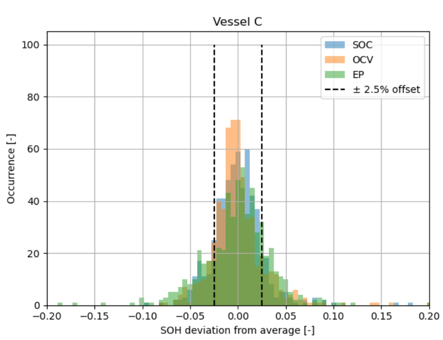

Figure 9. Histogram of the scattering of the methods estimation compared to the running average. The dashed black lines indicate the aspired precision limits.

The unsatisfying mostly mismatching estimates show a very questionable accuracy and a clear lack in precision. This makes further development necessary. Contrariwise, success seems not guarantied since the voltage signal might not provide enough significant information for a reliable execution of the OCV- or EP-based process. A longer, purposeful selected analysis window might be an improvement over a daily estimate. The scattered results also point to an over-fitting issue. But the model is well selected and has a good theoretical background. Therefore, regularization would be a constructive countermeasure against the spreading. These two points should be considered in future activities before a conclusive verdict can be rendered. The methods advantages like minimal prior knowledge and the possibility to obtain more then just the SOH (LLI, LAM, internal resistance), that in turn allows an assessment of the ability to provide power (not just capacity like SOH) or a better forward-looking SOH prediction, justify further ambitions.

In the following subsection, an extension of this method based on extensive characteristics tests to account for variations in current and temperature, among other things, will be presented.

3.4. Methods Based on Equivalent Circuit Models and Extensive Characteristics Tests

Equivalent circuit models (ECM) are often employed in battery management systems (BMS) due to their easy implementation and computational efficiency. They rely on experimental protocols to estimate cell properties such as the correlation between Open Circuit Voltage (OCV) and State Of Charge (SOC), and internal resistance. Nevertheless, the experimental and computational burden associated with implementing such models are significantly smaller than more complex models such as single particle models and Doyle-Fuller-Newman models.

ECMs represent the instantaneous and transient processes inside a lithium ion battery using circuit elements. Such a model is presented in Figure 10. The open circuit voltage of the cell is generated by the OCV element and the internal Ohmic resistance by the R_0 resistor. $R_1|C_1$ and $R_2|C_2$ represent transient processes in the cell at different timescales. T contains a thermal model, and h represents hysteresis effects when the values of the other elements may depend on the charge and discharge history of the cell.

The cell ECM defines a set of five *states*, (7), where SOC is cell *state of charge*, and U_1 and U_2 is the voltage drop over $R_1|C_1$ and $R_2|C_2$, respectively. h and T is the previously mentioned cell hysteresis level and cell temperature.

$$\mathbf{x} = \begin{bmatrix} SOC \\ U_1 \\ U_2 \\ h \\ T \end{bmatrix} \tag{7}$$

Each circuit element depend on the cell states and conditions. *E.g.*, the open circuit voltage and internal resistance typically depend on SOC, SOH, T, and h, and this may be modelled with lookup tables or estimated from real data.

The cell voltage and the overpotential (OP) are given by (8)

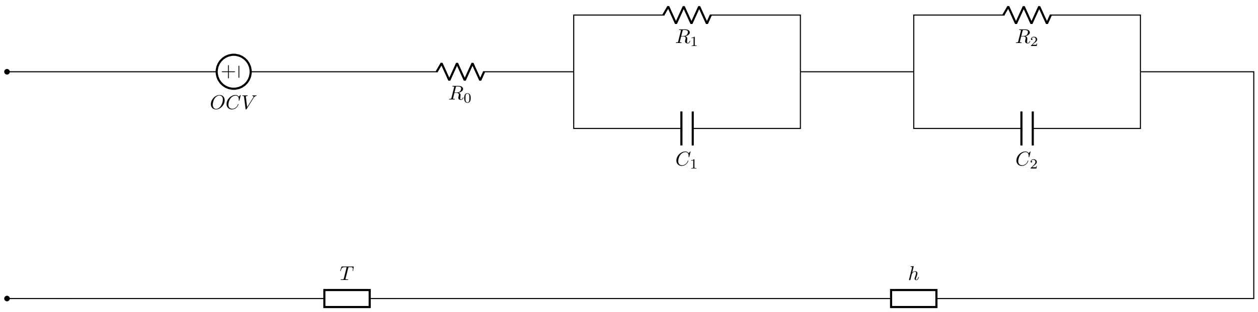

Figure 10. Schematic overview of an equivalent circuit model, containing an open circuit voltage element (OCV), cell internal resistance (R_0), transient processes ($R_1|C_1$ and ($R_2|C_2$)), an hysteresis model (h) and a thermal model (T).

and (9)

$$V = OCV\left(\mathbf{x}\right) + OP \tag{8}$$

$$OP = IR_0\left(\mathbf{x}\right) + U_1 + U_2 \tag{9}$$

The states change according to a set of differential equations, (10), where I is the cell current, η is the Coulombic efficiency of the cell, C_{nom} is the nominal capacity of the cell, α and β are parameters of the thermal model, T_a is the ambient temperature surrounding the cell and f_h is a function defining the cell hysteresis model. R_1, R_2, τ_1 and τ_2 are the resistances and time-constants of $(R_1|C_1)$ and $(R_2|C_2)$ presented previously in Figure 10. R_0 is the electrical resistance in the cell.

$$\frac{\partial \mathbf{x}}{\partial t} = \begin{bmatrix} \eta \frac{I}{SOH \times C_{\text{nom}}} \\ \frac{IR_1(\mathbf{x}) - U_1}{\tau_1(\mathbf{x})} \\ \frac{IR_2(\mathbf{x}) - U_2}{\tau_2(\mathbf{x})} \\ f_h\left(\mathbf{x}, I\right) \\ \alpha R_0\left(\mathbf{x}\right) I^2 - \beta\left(T - T_a\right) \end{bmatrix} \tag{10}$$

3.4.1. Method overview

The ECM-based SOH analysis is based on the estimation of the states OP and h which allows the lookup of SOC, and hence calculating the depth of discharge $DOD = SOC_2 - SOC_1$ and consequently the actual capacity from Coulomb counting. Integrating (10) between two SOC values leads to the correlation

$$SOH \times C_{\text{nom}} \times (SOC_2 - SOC_1) = \eta \times \int_{t(SOC_1)}^{t(SOC_2)} I \, \mathrm{d}t \tag{11}$$

which one may use to estimate SOH. Unlike the BMS, the algorithm presented herein runs offline; It makes use of the large available data to clean and filter out unnecessary data points and find the optimal anchor points that guarantee the most accurate SOH estimation. Besides, the computational limitations do not pose a problem. The ECM based algorithm consists of the following steps:

1. Initialization: prepare the lookup tables; configure the analysis; get the battery system size and units.
2. In a user-guessed period, query the pack-current data and find the optimal data analysis window.
3. Query and synchronise the voltage and temperature data for all cells within the pack; verify the data quality, then clean and correct the data.
4. Identify the optimal anchor points for the top charge and discharge cycles; *i.e.* deepest peak-to-peak Coulomb counting, most relaxed $min(OP)$, shortest duration, and most converged $|h| \rightarrow 1$.
5. Estimate state priors $\tilde{OP}(t)$, $\tilde{h}(t)$, $\tilde{OCV}(t)$, and $\tilde{SOC}(t)$ using the anchor points and SOC-independent ECM simulation through $\overline{R_0(SOC)}$, $\overline{R_1(SOC)}$, $\overline{R_2(SOC)}$, $\overline{C_1(SOC)}$, and $\overline{C_2(SOC)}$.
6. Simulate the ECM and calculate the posteriors $OP(t)$, $h(t)$, $OCV(t)$, $SOC(t)$, and SOH.
7. Calculate the confidence intervals using all sources of data and model inaccuracies through error propagation.

3.4.2. Verification on operational field data

In this section we consider data from operational systems in field. This is key in the evaluation strategy, as it allows us to capture any implications that only arise in field, e.g. related to operational constraints, data quality etc. In total, we have validated the ECM based SOH calculation in field against lab capacity checkup for 64 cell-pairs. They originate form 6 different modules at 5 different sites.

For field data evaluation, we do the following steps:

1. Calculate SOH from operational data in field for selected modules
2. Fetch those modules from the field and send them to one of Corvus's research labs.

3. Run the field return modules through lab capacity checkups (100 % to 0 % SOC)
4. Compare the SOH calculated form operational data with the SOH from the capacity checkup in lab.

Field validation scenario #1

Here we consider a module from a hybrid ferry which got 79.7 % SOH in the lab capacity checkup. The ECM based SOH was calculated from operational data one month earlier. The SOH was calculated on a cycle with DoD in the range 40 - 50 %. The ECM based SOH for the module was 79.7 %. The timeline of the process is show in Figure 11

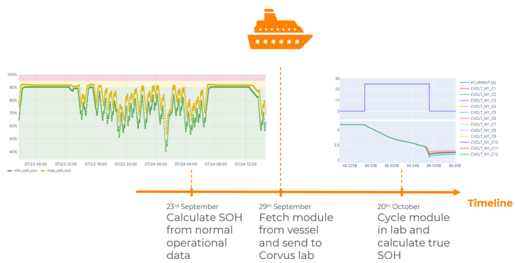

Figure 11. Timeline of the field return process in validation scenario 1

The module SOH is given by the lowest cell SOH in the module. Figure 12 compares the individual SOH results for each cell in the module. SOH estimated from operational data was lower than what was obtained in the lab for 9/12 cells. The cell with the largest error underestimated the actual SOH with 1.1 %.

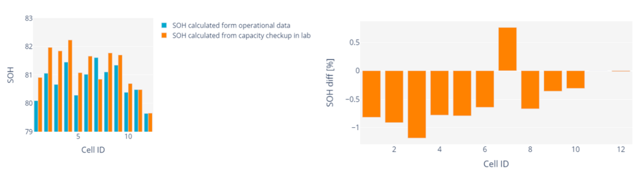

Figure 12. Results from field validation scenario 1. Estimation from operation data underestimated SOH in 9/12 cells when compared to results obtained in the lab.

Field validation scenario #2

Here we consider a module from a hybrid bulk carrier vessel which got 93.25 % SOH in the lab capacity checkup. Figure 13 compared the SOH values calculated from operational data and in the lab. The ECM based SOH was calculated from operational data one week before the module was fetched from field. In this scenario, the vessel performed a deep discharge and charge according Corvus SOH field test procedure, cycling the system from 80 % SOC to 20 % SOC with 15 min zero-current rest periods between the discharge and charge. The ECM based SOH for the module was 93.50 % SOH. The cell with the largest error underestimated the actual SOH with 0.3 %. SOH estimated from operaitonal data was underestimated in 8/12 cells.

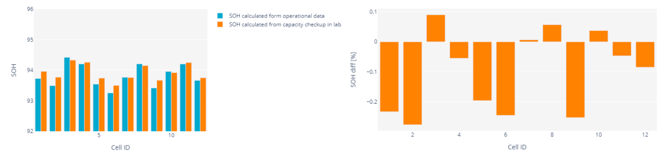

Figure 13. Results from field validation scenario 2. SOH-estimation from operational data underestimated SOH compared to lab-measurements in 8/12 cells.

Field validation scenario #3

Here we consider a module from the same vessel as in the second scenario. The SOH-values estimated from operational- and lab data are show in Figure 14. This module got 92.38 % SOH in the lab capacity checkup. The module is from the same vessel as field validation scenario #2. The ECM based SOH for the module was 92.85 % SOH. The cell with the largest error underestimated the actual SOH with 0.9 %.

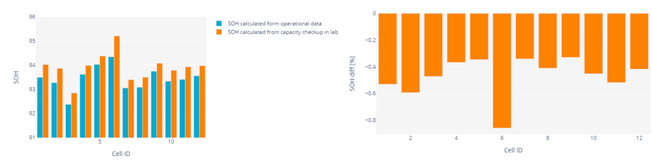

Figure 14. Results from field validation scenario 3. Estimation from operational data underestimated SOH in all cells.

Field validation scenario #4

Here we consider a module from a shore station. The module was disassembled in the lab, and four cells were tested individually. The resulting SOH error was in the range 1- 2 %.

Field validation scenario #5

Here we consider a module from a fully electric ferry which got 83.8 % SOH in the lab capacity checkup. Figure 15 compares the SOH values calculated in the lab capacity checkup to those calculated using the ECM model. There was a delay of more than 6 months between the last available field data and the lab capacity checkup The delay was due to first the pack being disconnected for 6 months (hence no cycles to calculate SOH), before it was fetched from field and was stored for additional months before the capacity checkup in lab was completed. The module was replaced due to deviating voltages on cell pair 12. As expected, the ECM based SOH calculated higher SOH values, especially on cell pair 12. A defect in this cell pair may cause accelerated degradation, possibly explaining the larger error between ECM based SOH and lab capacity checkup. The example illustrates the importance of a short delay between SOH calculation on operational data

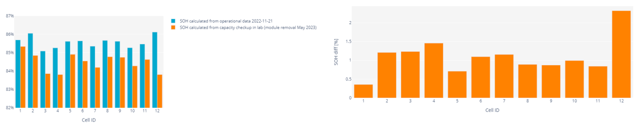

Figure 15. Results from field validation scenario 5. Estimation from operational data overestimated SOH in all cells. Almost 1 year storage of module between ECM based SOH calculation and lab capacity checkup.

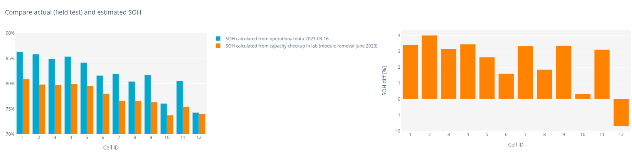

Figure 16. Results from field validation scenario 6. Estimation from operational data underestimated SOH in all cells. Almost 1 year storage of module between ECM based SOH calculation and lab capacity checkup.

and lab capacity checkup, despite practical difficulties in retrieving modules from field.

Field validation scenario #6

Here we consider a module from a shore station which got 73.7 % SOH in the lab capacity checkup. The ECM based SOH values presented in Figure 16 was calculated on operational data (DOD 40 %) over a period of almost 9 months, resulting in an estimated value of 76.1 %. This scenario highlights that the uncertainty of the result increase as the available data for the ECM calculation has lower DoD.

4. DISCUSSION

The results in this paper has demonstrated that by carefully constructing data-driven methods that exploits fundamental physical knowledge and utilizes results from extensive characterization tests, it is possible to obtain accurate and reliable capacity estimation based on collected sensor data without additional training of the data-driven models. Previous studies have shown that purely data-driven approaches might not be sufficiently accurate Vanem, Liang, Ferreira, et al. (2023), but by combining data-driven methods with the physical principle of Coulomb counting and an appropriate equivalent circuit model, results can be improved significantly, see also the summary in Vanem et al. (2024).

The simple linear model based on Coulomb counting is very attractive, since it needs not be trained and it can be used on snapshots of the data. However, it turned out difficult to get sufficiently accurate results, most likely due to the dependence on SOC and the uncertainties associated with this derived quantity. Ensemble methods and various filters could improve the results, but the dependency on SOC remains challenging. To avoid the strong dependence of SOC, an extended method that rather relates capacity to OCV was developed. This method utilizes a simple ECM to estimate OCV from voltage measurements during cycling. Then, an OCV-SOC curve is used to fit the estimated OCV and estimate capacity. All model parameters in such a model can be fitted based on snapshots of the data, and the only prerequisite is that the OCV-SOC curve is known. This can be found from characterization tests. Initial results with this method yield variable results, although average predictions are reasonable. However, by supplementing such an approach by comprehensive look-up tables from characterization tests to account for temperature and current effects, and by carefully fine-tuning the ECM model, reasonable SOH estimates can be obtained. This approach provides reasonable estimates from operational data provided that deep enough cycles are included in the data. Hence, this approach can be used to improve the annual capacity test, which may be performed based on normal operational data without requiring a specific test protocol or disruption of operations. Some requirements regarding DOD might be needed, but this can presumably be achieved during normal operation. In summary, this is believed to be the most promising method explored in this research, and it can be proposed for data-driven verification of SOH for ship classification. In fact, this method has already been used in actual verification of capacity for electrical ships in operation, as presented in a recent press release[1].

The provided comparisons of SOH estimated from field data and from lab measurements highlight the importance of high depth of discharge (DOD) for accurate estimation. Estimation from a DOD around 60% resulted in errors below 1%, while a DOD of 40% give errors up to 3%. An important contribution to the inverse relationship between DOD and accuracy may be the nonlinear nature of $\frac{\partial Q}{\partial OCV}$. Two voltage intervals may contain different amounts of charge, despite the voltage windows being equally wide. Consider two equally wide voltage windows ΔV_1 and ΔV_2 containing 60% and 30% of the total cell capacity respectively. In ΔV_1, information about 60% of the cell capacity is available, while ΔV_2 contain only 30% if the total information. Even if a cell has lost almost all the capacity in ΔV_2, it may retain almost all the capacity stores within ΔV_1.

5. SUMMARY AND CONCLUSION

This paper has presented various physics-informed data-driven approaches for diagnostics and state of health prediction for maritime battery systems. This is needed in order to satisfy classification requirements and to ensure the safety of electric ships. Previous studies have shown that purely data-driven methods, including cumulative methods, snapshot models and semi-supervised learning approaches might

[1] https://corvusenergy.com/corvus-energy-first-marine-ess-supplier-to-enable-data-driven-state-of-health-test-soh/

not be sufficient, and that they need to be combined with physics-based knowledge and models.

By doing this in a clever way, however, it is possible to develop methods that can be used based on sensor data from normal operation to replace the annual capacity test. The method proposed in this paper employs an equivalent circuit model and Coulomb counting together with extensive look-up tables from characterization tests and snapshots of sensor data collected during normal operation. It accounts for the effect of varying temperature, current and voltages and can therefore relax the strict requirements of the test protocols for the annual tests. The only requirement is that some relatively deep charge and discharge cycles are experienced during the operation. This represents a significant advantage over current capacity tests, which imposes disruptions of normal operations.

The method proposed in this paper has been tested and verified to perform satisfactorily on various case studies. Notwithstanding, further validation is recommended to strengthen the trust in this method, particularly for batteries approaching their end of life. Moreover, further testing and verification is required before applying the methods on different battery chemistries. Nevertheless, the method presented in this paper represent an improved way of performing the verification of SOH as required by classification societies, that offers considerable benefits for operators of electric ships.

ACKNOWLEDGMENT

This work has partly been partly carried out within the DDD BATMAN project, supported by MarTERA and the Research Council of Norway (project no 311445), and partly within the Sea Zero project, supported by the Research Council of Norway (project no 340898).

REFERENCES

Berecibar, M., Gandiaga, I., Villarreal, I., Omar, N., Van Mierlo, J., & Van den Bossche, P. (2016). Critical review of state of health estimation methods of li-ion batteries for real applications. *Renewable and Sustainable Energy Reviews*, *56*, 572-587.

Bertinelli Salucci, C., Bakdi, A., Glad, I. K., Vanem, E., & De Bin, R. (2023). A novel semi-supervised learning approach for State of Health monitoring of maritime lithium-ion batteries. *Journal of Power Sources*, *556*, 232429.

Bian, X., Liu, L., Yan, J., Zou, Z., & Zhao, R. (2020). An open circuit voltage-based model for state-of-health estimation of lithium-ion batteries: Model development and validation. *Journal of Power Sources*, *448*, 227401.

Bian, X., Wei, Z., Li, W., Pou, J., Sauer, D. U., & Liu, L. (2022). State-of-health estimation of lithium-ion batteries by fusing an open cirvuit voltage model and incremental capacity analysis. *IEEE Transactions on Power Electronics*, *37*(2), 2226-2236.

Birkl, C. R., Roberts, M. R., McTurk, E., Bruce, P. G., & Howey, D. A. (2017). Degradation diagnostics for lithium ion cells. *Journal of Power Sources*, *341*, 373-386.

Chen, L., Bao, X., Lopes, A. M., Xu, C., Wu, X., Kong, H., ... Huang, J. (2023). State of health estimation of lithium-ion batteries based on equivalent circuit model and data-driven method. *Journal of Energy Storage*, *73*(D), 109195.

Grindheim, C. A., Stakkeland, M., Glad, I. K., & Vanem, E. (2024). Comparative study of machine learning methods for state of health estimation of maritime battery systems. *Journal of Offshore Mechanics and Arctic Engineering*, *in press*.

Hill, D., Agarwal, A., & Gully, B. (2015). A review of engineering and safety considerations for hybrid-power (lithium-ion) systems in offshore applications. *Oil and Gas Facilities*, *4*(3), 68-77.

Hu, W., & Qian, Q. (2024). Lithium-ion battery state of health and failure analysis with mixture weibull and equivalent circuit model. *iScience*, *27*(6), 109980.

Huixin, T., Qin, P., Li, K., & Zhao, Z. (2020). A review of the state of health for lithium-ion batteries: Research status and suggestions. *Journal of Cleaner Production*, *261*, 120813.

Kejvalova, A. (2022). *Total least squares estimation of maritime battery capacity* (Master's thesis). Department of Mathemathics, University of Oslo.

Li, Y., Liu, K., Foley, A. M., Zülke, A., Berecibar, M., Nanini-Maury, E., ... Hoster, H. E. (2019). Data-driven health estimation and lifetime prediction of lithium-ion batteries: A review. *Renewable and Sustainable Energy Reviews*, *113*, 109254.

Liang, Q., Vanem, E., Alnes, Ø., Xue, Y., Zhang, H., Lam, J., & Bruvik, K. (2023). Data-driven state of health monitoring for maritime battery systems – a case study on sensor data from a ship in operation. *Ships and Offshore Structures*, *Latest articles*, 1-13.

Lipu, M. H., Hannan, M., Hussain, A., Hoque, M., Ker, P. J., Saad, M., & Ayob, A. (2018). A review of state of health and remaining useful life estimation methods for lithium-ion battery in electric vehicles: Challenges and recommendations. *Journal of Cleaner Production*, *205*, 115-133.

Meng, J., Boukhnifer, M., & Diallo, D. (2020). Comparative study of lithium-ion battery open-circuit-voltage online estimation methods. *IET Electrial Systems in Transportation*, *10*(2), 162-269.

Noh, T.-W., Kim, D. H., & Lee, B. K. (2023). Online state-of-health estimation algorithm for lithium-ion batteries in electric vehicles based on compression ratio of open circuit voltage. *Journal of Energy Storage*, *57*, 106258.

Pastor-Fernández, C., Yu, T. F., Widanage, W. D., & Marco, J. (2019). Critical review of non-invasive diagnosis techniques for quantification of degradation modes in lithium-ion batteries. *Renewable and Sustainable Energy Reviews*, *109*, 138-159.

Plett, G. L. (2011). Recursive approximate weighted total least squares estimation of battery cell total capacity. *Journal of Power Sources*, *196*, 2319-2331.

Shu, X., Shen, S., Shen, J., Zhang, Y., Li, G., Chen, Z., & Liu, Y. (2021). State of health prediction o flithium-ion batteries based on machine learning: Advances and perspectives. *iScience*, *24*(11), 103265.

Ungurean, L., Cârstoiu, G., Micea, M. V., & Groza, V. (2017). Battery state of health estimation: a structured review of models, methods and commercial devices. *International Journal of Energy Research*, *41*, 151-181.

Vanem, E., Alnes, Ø. Å., & Lam, J. (2021, November-December). Data-driven diagnostics and prognostics for modelling the state of health of maritime battery systems – a review. In *Proc. annual conference of the prognostics and health management society 2021 (phm 2021).*

Vanem, E., Bertinelli Salucci, C., Bakdi, A., & Alnes, Ø. Å. (2021). Data-driven state of health modelling – a review of state of the art and reflections on applications for maritime battery systems. *Journal of Energy Storage*, *43*, 103158.

Vanem, E., Bruch, M., Liang, Q., Reyes Gonzalez, D. V., & Alnes, Ø. Å. (2022, October-November). A data-driven snapshot method for state of health modelling and diagnostics of maritime battery systems. In *Proc. annual conference of the prognostics and health management society 2022 (phm 2022).*

Vanem, E., Bruch, M., Liang, Q., Thorbjørnsen, K., Valøen, L. O., & Alnes, Ø. Å. (2023). Data-driven snapshot methods leveraging data fusion to estimate state of health for maritime battery systems. *Energy Storage*, *5*(8), e476.

Vanem, E., Liang, Q., Bruch, M., Bøthun, G., Bruvik, K., Bakdi, A., … Agrell, C. (2023). *Statistical models for battery state of health* (Technical report No. 2023-1235). DNV.

Vanem, E., Liang, Q., Bruch, M., Bøthun, G., Bruvik, K., Thorbjørnsen, K., & Bakdi, A. (2024). Statistial models for condition monitoring and state of health estimation of lithium-ion batteries for ships. *Journal of Dynamics, Monitoring and Diagnostics*, *3*, 11-20.

Vanem, E., Liang, Q., Ferreira, C., Agrell, C., Karandikar, N., Wang, S., … Kandepu, R. (2023, October-November). Data-driven approaches to diagnostics and state of health monitoring of maritime battery systems. In *Proc. annual conference of the prognostics and health management society 2023 (phm 2023).*

Wang, L., Sun, J., Cai, Y., Lian, Y., Jin, M., Zhao, X., … Chen, J. (2023). A novel OCV curve reconstruction and update method of lithium-ion batteries at different temperatures based on cloud data. *Energy*, *268*, 126773.

Weng, C., Sun, J., & Peng, H. (2014). A unified open-circuit-voltage model of lithium-ion batteries for state-oc-charge estimation and state-of-health monitoring. *Journal of Power Sources*, *258*, 228-237.

Xiong, R., Li, L., & Tian, J. (2018). Towards a smarter battery management system: A critical review on battery state of health monitoring methods. *Journal of Power Sources*, *405*, 18-29.

Yang, H., Hong, J., Liang, F., & Xu, X. (2023). Machine learning-based state of health prediction for battery systems in real-world electric vehicles. *Journal of Energy Storage*, *66*, 107426.

Yu, Q.-Q., Xiong, R., Wang, L.-Y., & Lin, C. (2018). A comparative study on open circuit voltage models for lithium-ion batteries. *Chinese Journal of Mechanical Engineering*, *31*, 65:1-8.

Zhou, Z., Liu, Y., Zhang, C., Shen, W., & Xiong, R. (2024). Deep neural network-enabled battery open-circuit voltage estimation based on partial charging data. *Journal of Energy Chemistry*, *90*, 120-132.